P. Sguazzero

C. Chignoli

R. Rabagliati

G. Volpi

# Hydrodynamic Numeric Modeling of the Lagoon of Venice

Abstract: This paper describes two hydrodynamic numeric models and their application to the Lagoon of Venice, Italy. The models are based on the same mesh, bottom topography, boundary conditions, and spatial distribution of the bottom friction coefficient (Chézy coefficient). Although quite different in structure, both models ultimately provide sea level fluctuation and current speed at each meshpoint as functions of time. The first model numerically integrates the time-dependent, nonlinear, hyperbolic shallow water equations, written in conservation form, with a space-staggered leapfrog-type (time dense) scheme. The model is suited to episode simulation and is a particularly useful tool for system management and control. The second model is suited to long-term simulations and models only the astronomic tide; it solves a hybrid (differential-algebraic) system resulting from semilinearization of the shallow water equations under harmonic assumptions for the tide. Because of the superior computational efficiency of this second model, it has been used in conjunction with Powell's algorithm to identify the *a priori* unknown spatial distribution of the Chézy parameter. If the same Chézy distribution is fed into the two models, there can be obtained a complete, self-calibrating, consistent modeling tool for tidal basins with arbitrary geometric configurations and boundary conditions in the presence of hydraulic works.

### Introduction

Numerous theories have been advocated [1-5] in an attempt to provide tractable solutions to the equations governing tidal propagation in basins and coastal areas. With the advent of digital computers it has become customary to use numeric techniques in tidal calculations. Also, it has become feasible to model irregular bottom topographies, complicated geometric configurations and boundary conditions, and to include equation nonlinearities. The numeric methods fall naturally into two categories [6], harmonic methods and timestepping methods.

In the first class [7–9] there is assumed to exist *ab initio* a harmonic nature in the variations of the tidal characteristics with time, or more generally, a linear decomposition of these variations by means of a finite group of harmonic constituents. According to this assumption, the linearized tidal dynamics equations are reduced to a system of partial differential equations of elliptic type with respect to the complex amplitude of tidal oscillations of the sea level. The formulated boundary-value problem has a unique solution (under suitable conditions on the angular velocities of the tidal wave and on the Coriolis parameter) if the values of the amplitudes are known on a part of the boundary of the body of water, while on the other part

there is a condition of no flow [6]. The solution is then found by standard numeric methods for elliptic problems [10]; mild nonlinearities in the original tidal dynamics equations can be treated by iterating the procedure just described [5]. The primary output of harmonic methods is given by the complex amplitudes of the harmonic constituents of the sea level as functions of space; current velocity and water depth, as functions of space and time, are hence obtained by Fourier synthesis.

In the timestepping methods no *a priori* assumptions are made about the nature of the time variations of the tide. Instead, arbitrary initial conditions are set for water depths and velocities. No-flow or no-slip conditions are also prescribed at the sea-land boundary, while at the seaward boundary the vertical tide is given. The integration of the time-dependent, nonlinear, hyperbolic tidal dynamics equations is then carried out numerically in a stepwise manner by using well known finite difference [2, 6, 11–22] or finite element [23] techniques. The current velocity and water depth are obtained directly at discrete intervals in space and time.

It is the purpose of this paper to illustrate how the two methodologies can be consistently integrated in order to build models of tidal propagation that are less subject to

**Copyright** 1978 by International Business Machines Corporation. Copying is permitted without payment of royalty provided that (1) each reproduction is done without alteration and (2) the *Journal* reference and IBM copyright notice are included on the first page. The title and abstract may be used without further permission in computer-based and other information-service systems. Permission to *republish* other excerpts should be obtained from the Editor.

limitations associated with definition of the bottom friction parameter (Chézy parameter C) necessary for the solution. One distinct advantage of such a procedure is that both immediate and long-term effects of modifications of the physical system to be modeled can be analyzed by appropriate means. For instance, permanent changes in the geometric configuration can be rapidly analyzed by the harmonic method, while episode simulation and computations of extremal values (high and low water levels, maximum velocities) are best carried out by the nonlinear time-dependent method. These methods have been specifically applied to the Lagoon of Venice, Italy. In particular, a proposal to construct engineering works at the inlets of the lagoon (Fig. 1) raised many questions regarding the effects such works would have on the hydraulics of the system. Many considerations are involved, and a number of investigations from various standpoints were undertaken both at the IBM Venice Scientific Center (VSC) [24–29] and by other research groups [9, 30–32]. The studies at VSC were centered on a nonlinear, timedependent numeric model of the shallow water flow in the lagoon. In addition, a second harmonic-type numeric model was applied, the principal function of which was to play a supporting role to the nonlinear model.

The mathematical techniques developed in constructing the numeric models are presented in the first two parts of this paper. The way in which the harmonic model provides essential support to the nonlinear model is then described, and finally, a summary of the applications and results of the models is given.

# Time-dependent nonlinear model

## • Basic equations for shallow water flow

In a partly enclosed basin of small size, tidal motions are formed by interaction of horizontal gradient forces, inertial forces, Coriolis forces, and bottom friction. Since in this paper we make application exclusively to a system of small scale and shallow water depth, where frictional forces are dominant, we can neglect the effect of earth rotation [18]. On the other hand, the nonlinear momentum advection is included. Within the basin domain the vertically integrated equations of motion and continuity in the divergence form [33–35] are

$$\frac{\partial U}{\partial t} + \frac{\partial}{\partial x} (Uu) + \frac{\partial}{\partial y} (Uv) 
+ g\zeta \frac{\partial \eta}{\partial x} + \frac{g}{C^2} \left( \frac{QU}{\zeta^2} \right) = 0, \qquad (1)$$

$$\frac{\partial V}{\partial t} + \frac{\partial}{\partial x} (Vu) + \frac{\partial}{\partial y} (Vv) 
+ g\zeta \frac{\partial \eta}{\partial y} + \frac{g}{C^2} \left( \frac{QV}{\zeta^2} \right) = 0, \qquad (2)$$

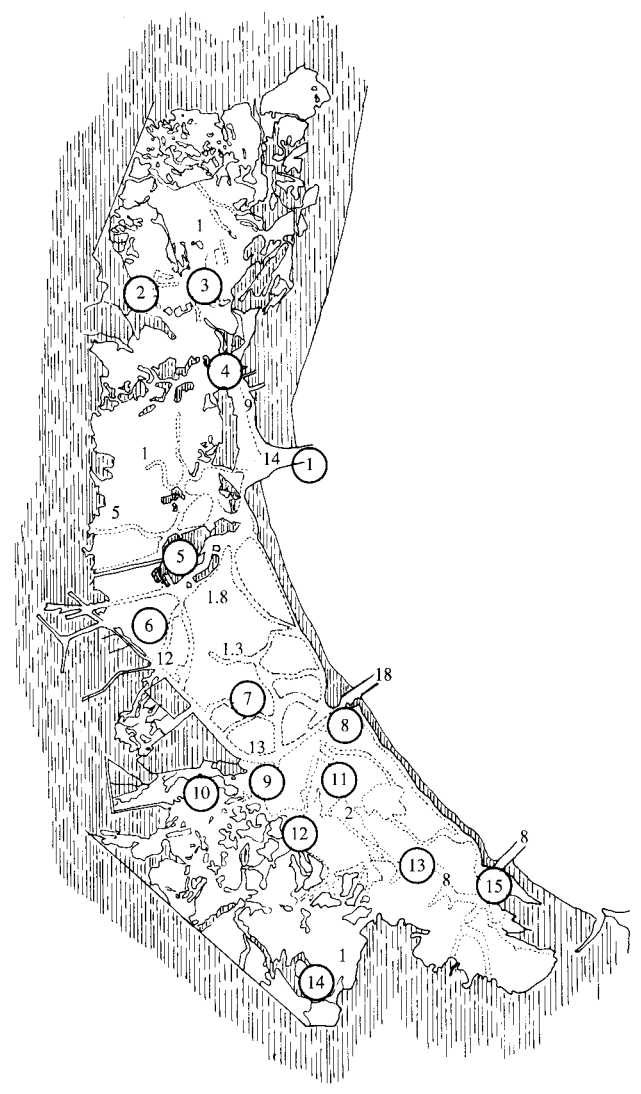


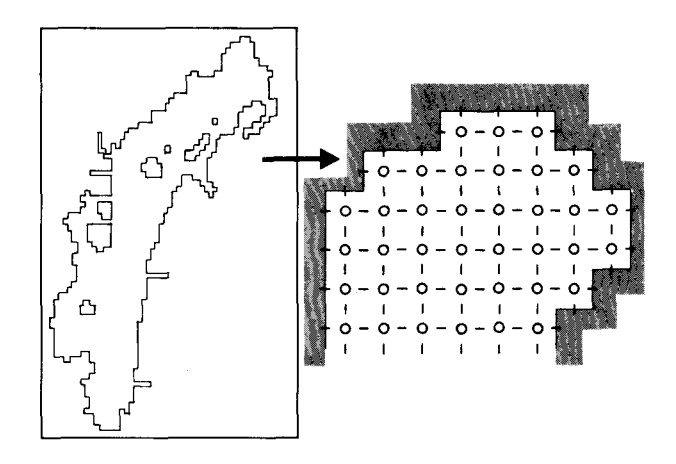
Figure 1 The Lagoon of Venice. Typical values of depth (in m) are reported. The oceanographic stations whose data were used in this work are also shown; Venice is station no. 5.

and

$$\frac{\partial \zeta}{\partial t} + \frac{\partial U}{\partial x} + \frac{\partial V}{\partial y} = 0, \tag{3}$$

in which x and y are horizontal Cartesian coordinates; t is the time; U(x, y, t) and V(x, y, t) are the respective vertically integrated x and y components of transport per unit width; g is the gravity;  $\eta(x, y, t)$  is the water level elevation relative to the local mean sea level (msl) datum;  $\zeta(x, y, t)$  is the water depth at position x, y and time t, and  $\zeta = \eta + H$ , where -H(x, y) is the elevation of the sea bed relative to the msl datum;  $u = U/\zeta$  and  $v = V/\zeta$ ; and  $Q = (U^2 + V^2)^{1/2}$  is the magnitude of the transport per unit

473



Kind of point	Coordinates	Defined values	Computed values			
	$l\Delta s, \left(m-\frac{1}{2}\right)\Delta s$	Н	$C, U, \bar{u}, \mu_x \eta, \mu \bar{v}$			
1	$\left(i-\frac{1}{2}\right)\Delta s, m\Delta s$	H	$C, V, \bar{v}, \mu_y \eta, \mu \bar{u}$			
0	$\left(t-\frac{1}{2}\right)\Delta s, \left(m-\frac{1}{2}\right)\Delta s$	η (inlets only)	η (internal points only)			

Figure 2 Staggered mesh system.

width. It must be noted that the frictional effects of turbulence are represented only by a bottom stress vector  $\tau$  in the quadratic form

$$\tau = -\left(\frac{g}{C^2}\right) \frac{Q}{\zeta^2} \quad (U, V), \tag{4}$$

where C is a bottom friction coefficient (Chézy coefficient) the determination of which requires special attention [2-3].

## • Initial and boundary conditions

In order to get a well defined mathematical formulation, Eqs. (1)-(3) must be supplemented by initial and boundary conditions. Due to the friction, the influence of initial conditions disappears as the computation progresses; thus, we can freely set  $U=V=\eta=0$  at t=0. With regard to the boundary conditions, we will set to zero the normal component of the transport at the sea-land boundaries  $\gamma_1$ , prescribing the elevation  $\eta$  as a function of time at the open (seaward) boundary  $\gamma_0$ .

#### • Formulation of difference equations

A number of numeric techniques are available to solve Eqs. (1)-(3) when they are supplemented by boundary and initial conditions [2, 6, 11-22, 36]. Following [15], we

adopt a finite-difference, leapfrog type (time-dense) numeric scheme [37] that is explicit, space-staggered, and second-order-accurate. In this scheme the values of U, V, and  $\zeta$  are evaluated for uniform time steps  $\Delta t$  on a uniform Cartesian mesh (see Fig. 2) of spacing  $\Delta s$ , which covers the computational domain  $\Omega$ ;  $\zeta_{l,m}^n$  is regarded as representative of  $\zeta[(l-1/2)\Delta s, (m-1/2)\Delta s, n\Delta t]$ , where l, m, and n are integers; U is evaluated at  $t = n\Delta t$ ,  $x = l\Delta s$ , and  $y = (m-1/2)\Delta s$ ; V is evaluated at  $t = n\Delta t$ ,  $t = (l-1/2)\Delta s$ , and  $t = m\Delta t$ . By using these notations and the conventions

$$\delta_x f_{l,m} = f_{l+1/2,m} - f_{1-1/2,m},\tag{5}$$

$$\delta_{y} f_{l,m} = f_{l,m+1/2} - f_{l,m-1/2}, \tag{6}$$

$$\mu_x f_{l,m} = \frac{1}{2} \left( f_{l+1/2,m} + f_{l-1/2,m} \right), \tag{7}$$

$$\mu_{\nu}f_{l,m} = \frac{1}{2} (f_{l,m+1/2} + f_{l,m-1/2}),$$
 (8)

$$\mu = \mu_x \mu_y,\tag{9}$$

$$D_x f_{l,m} = f_{l+1,m} - f_{l-1,m}, (10)$$

and

$$D_{y}f_{l,m} = f_{l,m+1} - f_{l,m-1}, (11)$$

we define the finite difference analogs of Eqs. (1)-(3) as

$$U^{n+1} - U^{n-1} + p\{D_x(U\bar{u}) + \mu(\bar{v})D_yU + 2U\delta_y[\mu_x(\bar{v})] + 2g\mu_x(\zeta)\delta_x\eta\}^n + \frac{2g\Delta t}{C^2} \bar{u}^{n+1}\bar{q}^{n-1} = 0,$$
 (12)

$$V^{n+1} - V^{n-1} + p\{\mu(\bar{u})D_xV + 2V\delta_x[\mu_y(\bar{u})] + D_y(V\bar{v})$$

$$+ 2g\mu_{y}(\zeta)\delta_{y}\eta\}^{n} + \frac{2g\Delta t}{C^{2}} \bar{v}^{n+1}\bar{q}^{n-1} = 0,$$
 (13)

and

$$\zeta^{n+1} - \zeta^{n-1} + 2p(\delta_x U + \delta_y V)^n = 0, \tag{14}$$

where  $p = \Delta t/\Delta s$ , and  $\zeta^n$  refers globally to all values  $\zeta^n_{l,m}$ ; similar definitions apply to  $U^n$  and  $V^n$ ; moreover,  $\bar{u}$  stands for  $U/\mu_x\zeta$ ,  $\bar{v}$  stands for  $V/\mu_y\zeta$ , and  $\bar{q} = [\bar{u}^2 + (\mu\bar{v})^2]^{1/2}$  or  $[(\mu\bar{u})^2 + \bar{v}^2]^{1/2}$ , depending on the place. It should be noted that the friction terms in Eqs. (12) and (13), nominally centered at time  $t = n\Delta t$ , make explicit use (following [18]) of the values  $U^{n+1}$  and  $V^{n+1}$  to be predicted. This prevents the friction from causing unrealistic velocity inversions. Equations (12)–(14) provide a consistent, second-order-accurate, conditionally stable [19] approximation to Eqs. (1)–(3). The discussion on the application and results of these equations is deferred to a later section.

### Semilinear model

• Semilinearization of the shallow water equations Under the assumption that the elevation  $\eta$  is small with respect to H, the advective terms can be dropped [4] and Eqs. (1)-(3) change [1, 4, 14] into the semilinear system:

$$\frac{\partial U}{\partial t} + gH \frac{\partial \eta}{\partial x} = \tau_x, \tag{15}$$

$$\frac{\partial V}{\partial t} + gH \frac{\partial \eta}{\partial v} = \tau_y, \tag{16}$$

and

$$\frac{\partial \eta}{\partial t} + \frac{\partial U}{\partial x} + \frac{\partial V}{\partial y} = 0, \tag{17}$$

where  $\tau$  is the bottom stress vector;

$$\tau = -\frac{gQ}{C^2H^2} (U, V).$$
 (18)

A further simplification can be obtained by replacing the quadratic dissipation form (18) with the linear form

$$\tau = -r(U, V), \tag{19}$$

where r = r(x, y) is to be determined. Following in principle Refs. [2, 38], we substitute the solution vector  $(U, V, \eta)$  of Eqs. (15)–(17),(19) into Eqs. (15)–(18) to get the residual vector  $[(g/C^2)(UQ/H^2) - rU, (g/C^2)(VQ/H^2) - rV, 0]$ . If we now prescribe the orthogonality between this residual and the solution of Eqs. (15)–(17), (19) in the time interval  $(t_1, t_2)$ , we obtain the relation

$$\frac{g}{C^2H^2} \int_{t_1}^{t_2} Q^3 dt = r \int_{t_1}^{t_2} Q^2 dt, \qquad (20)$$

which links the dissipation coefficients C and r of the two forms, (18) and (19), and expresses the equivalence in the mean of the energies dissipated by (18) and (19) in the time interval  $(t_1, t_2)$ . We can heuristically conclude that the solution of the hybrid (differential-algebraic) system [Eqs. (15)-(17), (19), (20)] in the unknowns  $U, V, \eta$ , and r provides a solution (in a weaker sense) of the semilinear system (15)-(18), under the same initial and boundary conditions; therefore, we now investigate Eqs. (15)-(17), (19), (20).

## • Harmonic method

Following [2, 7, 9, 39], we assume a representation of the solution vector of Eqs. (15)–(17), (19), (20) by means of a finite group of harmonic constituents:

$$\eta(x, y, t) = \text{Re} \sum_{k=1}^{K} \hat{E}^{k}(x, y) \exp(i\omega_{k}t),$$
(21)

$$U(x, y, t) = \text{Re } \sum_{k=1}^{K} \hat{U}^{k}(x, y) \exp(i\omega_{k}t),$$
 (22)

and

$$V(x, y, t) = \text{Re} \sum_{k=1}^{K} \hat{V}^{k}(x, y) \exp(i\omega_{k}t),$$
 (23)

where  $\hat{E}^k$ ,  $\hat{U}^k$ ,  $\hat{V}^k$  and  $\omega_k$  are the complex amplitude and the angular frequency, respectively, of the kth component of the solution vector. It is easily seen that if we substitute Eqs. (21)-(23) in to Eqs. (15)-(17) we obtain

$$\frac{\partial}{\partial x} \left( f^k \frac{\partial \hat{E}^k}{\partial x} \right) + \frac{\partial}{\partial y} \left( f^k \frac{\partial \hat{E}^k}{\partial y} \right) + \omega_k^2 \hat{E}^k = 0,$$
for  $k = 1, 2, \dots, K$ , (24)

where

$$f^k = \frac{gH}{1 - i(r/\omega_k)} \,, \tag{25}$$

provided

$$\hat{U}^k = i \left( \frac{f^k}{\omega_k} \right) \frac{\partial \hat{E}^k}{\partial x},\tag{26}$$

and

$$\hat{V}^k = i \left( \frac{f^k}{\omega_k} \right) \frac{\partial \hat{E}^k}{\partial y}. \tag{27}$$

This is a system of K elliptic partial differential equations in the (complex) sea level oscillation amplitudes  $\hat{E}^k$ , coupled by the algebraic relation

$$r = \frac{g}{C^2 H^2} \left[ \int_t^{t_2} (U^2 + V^2)^{3/2} dt \right] \left[ \int_t^{t_2} (U^2 + V^2) dt \right]^{-1} (28)$$

and Eqs. (22)-(23), (25)-(27).

# • Boundary conditions

Since Eq. (24) does not need initial conditions, only the boundary conditions must be specified. They are

$$\hat{E}^k|_{\gamma_0} = \hat{E}^k_{\mathbf{A}} \tag{29}$$

on the seaward boundary  $\gamma_0$  (where the subscript A refers to the Adriatic Sea), while on the sea-land boundary  $\gamma_1$  the no-flow condition can be recast as

$$\frac{\partial}{\partial \nu} \left. \hat{E}^k \right|_{\gamma_1} = 0,\tag{30}$$

where  $\nu$  is the normal to the coastline.

# • Finite difference formulation

We solve Eqs. (21)-(30) numerically by finite difference, using the space-staggered grid discussed previously and centered, second-order-accurate formulae [40]. For instance, Eq. (24) has the numeric analog

$$[\delta_{x}(f_{l,m}\delta_{x}\hat{E}_{l,m}^{k})] + [\delta_{y}(f_{l,m}\delta_{y}\hat{E}_{l,m}^{k})] + (\Delta s)^{2}\omega_{k}^{2}\hat{E}_{l,m}^{k} = 0,$$
for  $(x_{l,m}, y_{l,m}) \in \Omega; k = 1, 2, \dots, K.$  (31)



Figure 3 Gray-tone map of the lagoon depth.

For fixed r = r(x, y) and  $f^k$  given by Eq. (25), the set of K sparse linear systems (31) can be solved by iterative methods [41-42] or, more efficiently, by direct methods. For instance, Gaussian decomposition techniques can be applied to sparse matrices [43] to significantly reduce execution time and storage requirements. Because  $r = r(x, y | \hat{E}^k, k = 1, \dots, K)$  is a nonlinear function of  $\hat{E}^k$  by virtue of Eqs. (21)-(23), (25)-(28), Eqs. (28) and (31) must be solved iteratively for given C = C(x, y) until convergence is reached. More exactly, the iterative process has the following steps:

- a. Guess the distribution r = r(x, y).
- b. Solve Eqs. (21)–(23), (25)–(27), (29)–(31) by direct methods with the last distribution of r.
- c. Get a new distribution of r by using

$$r_{N+1}(x, y)$$

$$= \frac{1}{2} [r_N(x, y) + r(x, y | \hat{E}_N^k, k = 1, 2, \dots, K)],$$
(32)

- where N is an iteration subscript,  $\hat{E}_N^k$  is the solution of Eq. (31) when  $r = r_N$ , and  $r(x, y | \hat{E}_N^k, k = 1, \dots, K)$  is given by Eqs. (22)-(23), (25)-(28).
- d. If the old and the new r distributions differ too much go to step b; otherwise exit.

## Identification of the Chézy coefficient

Wave motion in shallow areas is mainly influenced by bottom friction [18]. If Chézy's law (4) is chosen to represent the resistance, the determination of the Chézy coefficient C requires special care. The C values depend on the depth, shape, and composition of the bottom, and accurate field estimates of these parameters are difficult to obtain [2]. In the absence of direct measurements it is necessary to resort to simple schematization, e.g., the postulation of a logarithmic dependence of C on the depth [3, 15]:

$$C = a_1 \log (a_2 d), \tag{33}$$

where  $d = \zeta(x, y, t)$  for the nonlinear model, and d = H(x, y) for the semilinear model; or the postulation of a power law as in [24]. In any case we will be given a relation of the general form

$$C = C(d \mid a_1, a_2, \cdots, a_p), \tag{34}$$

where the  $a_q$ ,  $q=1,2,\cdots,p$ , are disposable parameters to be indirectly estimated from field data. The identification procedure can be conducted in principle on the nonlinear model; however, given the considerably greater computational efficiency of the semilinear model, we use the latter. Assume that we are given a set of observed tidal oscillation amplitudes  $\hat{\xi}_j^k$  for  $k=1,2,\cdots,K$  and  $j=1,2,\cdots,J$  at fixed locations  $P_j$  in our computational domain  $\Omega$ , and that we are required to estimate the unknown parameters  $a_q$ . As a natural error criterion we first choose the function

$$F(a_1, a_2, \dots, a_p)$$

$$= \sum_{j} \sum_{k} \left[ \hat{E}^k(P_j | a_1, a_2, \dots, a_p) - \hat{\xi}_{j}^k \right]^2, \tag{35}$$

where  $\hat{E}^k(P_j | a_1, a_2, \dots, a_p)$  is the solution of Eqs. (21)–(30), (34) in  $P_j$ , and then consider as optimal the  $a_q$  that minimize F.

Local minima of the function F can be obtained by iterative methods. Some of these, like the gradient method, make explicit use of the partial derivatives of F with respect to the parameters  $a_q$ , which in turn must be computed by introducing and solving an adjoint set of equations in the variables  $d\hat{E}^k/da_q$  [obtained formally by differentiating Eqs. (21)-(30), (34)] [44-46]. This is the procedure followed in [47] for a simpler case. Although very promising from a theoretical standpoint, this procedure requires cumbersome algebraic manipulations and

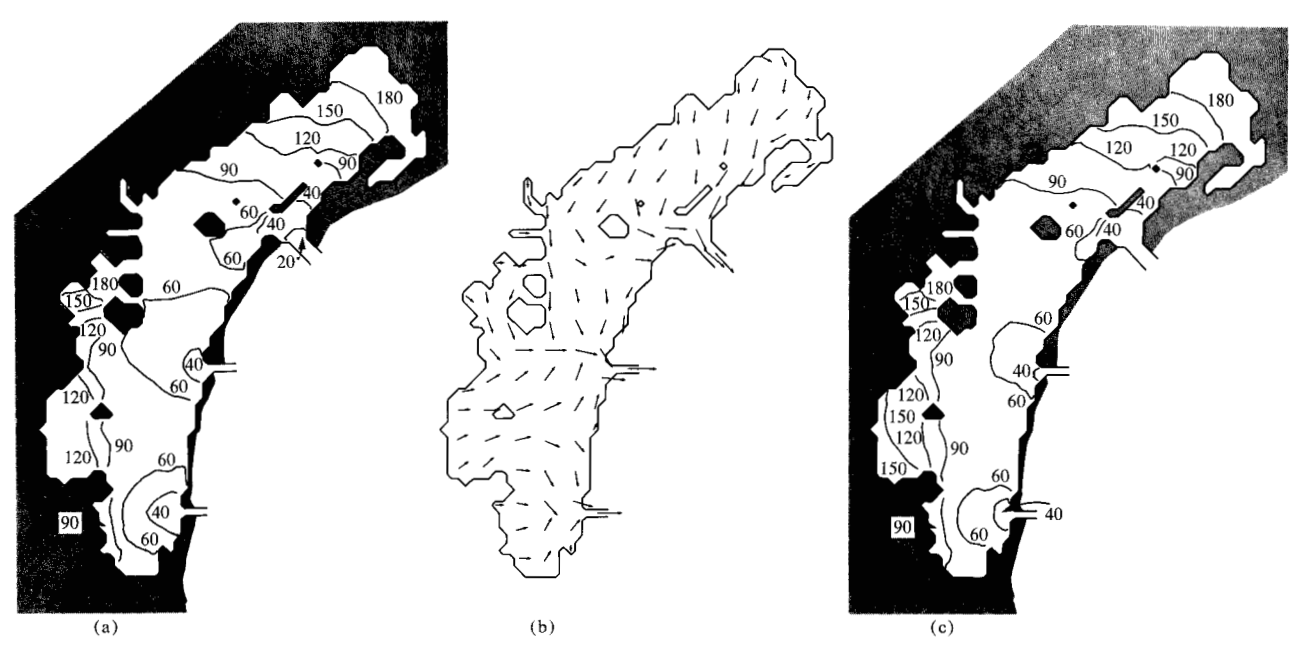


Figure 4 (a) Contour map of the phase delay (in minutes) of the  $M_2$  component. (b) Typical ebb tide velocity field. (c) Contour map of the phase delay (in minutes) of the  $M_2$  component corresponding to a permanent narrowing of the inlets ( $\lambda = 0.35$ ).

considerably increases the time-space computational complexity of the original problem. In practice, satisfactory results can be obtained with minimization algorithms (like Powell's algorithm) that do not make explicit use of the derivatives  $dF/da_a$  [48].

The complete procedure is summarized in four steps:

- a. Guess the parameter vector  $\mathbf{a} = (a_1, a_1, \dots, a_n)$ .
- b. Compute  $C(\mathbf{a})$  by Eq. (34).
- c. Solve Eqs. (21)-(23), (25)-(31).
- d. Exit if F is less than a prefixed tolerance; otherwise get a new parameter vector **a** by Powell's algorithm and go to step b.

#### Application of results

## • Description of the physical environment

The numeric models described in this paper have been applied to the Lagoon of Venice. The basin, which has a surface of about 450 km² and an average depth of about 1 m, is located in the northern part of the Adriatic Sea, at approximately 48° north latitude and 12° east longitude; it extends SW-NE about 50 km and about 10 km in the orthogonal direction, as shown in Fig. 1. The lagoon is connected with the Adriatic Sea through three inlets (Lido, Malamocco, and Chioggia); its complicated internal structure consists of a network of channels 2 to 18 meters deep that cut across large areas of very shallow waters (Fig. 3). Tidal propagation originates at the inlets and is mainly affected by bottom shape and roughness. Indeed, the tidal harmonic components inside the Lagoon are reduced in amplitude and delayed in phase [27] with respect

to the Adriatic Sea. The very thorough sea level fluctuation data, recorded by several oceanographic stations (shown in Fig. 1) during 1972 and 1973 and made available to us, have made use of the outlined technique possible.

### • Characteristics of the numeric models

The two numeric models are based on the same grid of 612.5 m size with 1201 meshpoints; they use the same bottom topography and the same Chézy coefficient. Both models use relation (33) with  $a_1 = 17.7$  and  $a_2 = 103.6$ , obtained by the calibrating procedure previously discussed.

The number K of tidal components in the relations (21)–(23) of the semilinear model, following [27, 49], is seven. These are grouped in two bands, of diurnal and semi-diurnal frequencies, respectively, and are conventionally designated as  $O_1$ ,  $P_1$ ,  $K_1$ ,  $N_2$ ,  $M_2$ ,  $M_2$ ,  $M_2$ , and  $M_2$ . The interval  $M_2$  of the relation (28) covers the two years (1972–1973) of available sea level data.

## • Results of the semilinear model

With the choice of  $a_1=17.7$  and  $a_2=103.6$  the relative root mean square (rms) deviation between the computed and observed astronomical tide amplitudes is less than 0.1. In Table 1 we show, for all stations, the values of the harmonic constants for the two most important components,  $M_2$  (of period 12 hr 25 min) and  $K_1$  (of period 23 hr 56 min). The relative rms errors are about 0.09 and 0.05, respectively. Figure 4(a) shows a contour map of the phase delay, with respect to the inlets, of the semidiurnal component  $M_2$ . Figure 4(b) shows a typical ebb tide velocity field (tidal current regime).

477

**Table 1** Harmonic constants  $(\rho, \phi)$  for components  $M_2$  and  $K_1$  at oceanographic stations;  $\rho^k \exp(i\phi^k)$  is the polar form of  $\hat{E}^k$ ;  $\rho_k^k \exp(i\phi_k^k)$  is the complex amplitude at the lagoon inlets; the Punta della Salute station is located in the city of Venice; circled numbers after the station names refer to Fig. 1.

Station		$\rho_{i}$	$/ ho_{_{ m A}}$	$\phi - \phi_A$ (in minutes)					
	M	$\mathbf{I_2}$	K	ζ,	M	$I_2$	<b>K</b> <sub>1</sub>		
	Computed	Observed	Computed	Observed	Computed	Observed	Computed	Observed	
Treporti 4	0.73	0.85	0.87	0.95	76	72	93	80	
Le Saline ③	0.62	0.74	0.82	0.86	130	135	153	156	
Pagliaga ②	0.74	0.72	0.88	0.85	148	149	164	172	
Punta Salute (5)	0.99	1.06	0.99	1.00	59	58	59	60	
S. Giorgio Alega 6	1.01	1.03	0.99	1.02	64	79	63	80	
Faro Rocchetta (8)	0.98	1.01	0.99	1.01	25	33	25	32	
Ex Poveglia ⑦	1.00	1.05	0.99	1.01	58	56	57	56	
Canale Melison (9)	0.99	1.00	0.99	0.99	55	65	54	68	
Torson di Sotto 10	1.00	1.03	0.99	1.00	57	69	56	68	
Valgrande (11)	0.97	0.98	0.98	0.98	64	69	64	72	
Settemorti 12	0.92	0.89	0.97	0.95	92	93	94	100	
Chioggia (15)	0.98	0.97	0.99	0.97	30	23	30	19	
Petta de Bo (13)	0.96	0.96	0.98	0.97	69	61	70	64	
Fogolana 14	0.88	0.77	0.95	0.95	146	136	150	152	

Table 2 Amplitude reduction  $r_e$  and time delay  $d_e$  for components  $M_2$  and  $K_1$ , at oceanographic stations, caused by narrowing of the inlets (varying  $\lambda$  values).

Station	$r_{ m e}$						$d_{ m e}$						
	$M_2$			$\mathbf{K}_{1}$			(in minut $M_2$			K <sub>1</sub>			
	$\lambda = 0.52$	0.35	0.17	0.52	0.35	0.17	$\lambda = 0.52$	0.35	0.17	0.52	0.35	0.17	
Treporti	0.97	0.89	0.59	0.99	0.96	0.79	3	12	43	4	17	78	
Le Saline	0.97	0.91	0.65	0.99	0.96	0.81	3	10	34	4	15	64	
Pagliaga	0.97	0.90	0.61	0.99	0.96	0.79	3	8	24	4	14	59	
Punta Salute	0.96	0.85	0.52	0.98	0.94	0.74	4	16	49	6	24	93	
S. Giorgio Alega	0.96	0.85	0.52	0.98	0.94	0.74	5	18	52	7	26	96	
Faro Rocchetta	0.94	0.82	0.49	0.98	0.93	0.73	9	28	79	11	37	122	
Ex Poveglia	0.95	0.85	0.52	0.98	0.94	0.74	6	21	60	8	29	103	
Canale Melison	0.95	0.84	0.52	0.98	0.94	0.74	7	23	64	9	31	106	
Torson di Sotto	0.95	0.85	0.53	0.98	0.94	0.74	7	23	64	9	31	106	
Valgrande	0.95	0.85	0.53	0.98	0.94	0.75	7	22	62	8	30	103	
Settemorti	0.96	0.86	0.56	0.98	0.95	0.76	6	20	53	7	27	92	
Chioggia	0.96	0.85	0.52	0.98	0.94	0.75	6	23	69	7	30	110	
Petta de Bo	0.96	0.86	0.54	0.98	0.94	0.75	6	21	60	8	28	99	
Fogolana	0.96	0.88	0.59	0.98	0.95	0.77	5	15	35	6	21	72	

After the calibration, the model can be used to predict the astronomical tide under different conditions, such as, for example, conditions following the construction of engineering works. One interesting problem is the assessment of the impact of reducing inlet cross sections (by means of new dams) on the tidal dynamics. The reduction can be simulated by suitable modification of the C values at the meshpoints involved in the restriction. As in [24, 50–51], the chosen relation between new  $(C_n)$  and old  $(C_o)$  values of C is

$$C_{\rm n} = \left[ \left( \frac{1}{C_{\rm o}} \right)^2 + \frac{H}{2g\Delta s} \left( \frac{b_{\rm o}}{C_{\rm c}b_{\rm n}} - 1 \right)^2 \right]^{-\frac{1}{2}},$$
 (36)

where  $C_{\rm c}$  is the so-called contraction coefficient;  $b_{\rm n}$  and  $b_{\rm o}$  are the respective new and old values of the inlet cross sections. Table 2 shows the amplitude reduction  $r_{\rm e}$  and the time delay  $d_{\rm e}$  (with respect to the original lagoon configuration) at the oceanographic stations for the two most important components,  $M_{\rm e}$  and  $K_{\rm l}$ , and three values of

the parameter  $\lambda = C_{\rm c} b_{\rm n}/b_{\rm o}$ . Similarly, the contour lines of the phase of  $M_2$  after the narrowing are reported in Fig. 4(c).

#### • Results of the time-dependent nonlinear model

The effectiveness of the time-dependent nonlinear model is best illustrated by its ability to show evolution of the flow field. Particularly interesting, as far as the Venice Lagoon is concerned, are the cases in which the forcing tide at the inlets cannot be represented by formulae like (21)-(23) due, for instance, to superposition of the meteorologic (wind-driven) and astronomic components. In such cases exceptionally high (or low) tides can be generated inside the lagoon. Figure 5 shows an episode of flooding of the city of Venice, as actually recorded (February 13, 1972), and as computed by the model. Figure 6 demonstrates how the flooding could have been avoided by suitably operating mobile sluices at the inlets of the Lagoon. On the other hand, the numeric simulations have clearly indicated that the flooding cannot be prevented by a permanent but incomplete narrowing of the inlets.

#### Summary

Two differently structured hydrodynamic numeric models of the Lagoon of Venice have been presented. One is a nonlinear model; the other is semilinear. Each can provide time-dependent values for sea level fluctuation and current velocity.

The nonlinear model is particularly useful for singleepisode simulation, whereas the semilinear model is best suited for long-term simulation problems and is much more computationally efficient.

This model has been used in conjunction with Powell's algorithm to identify the spatial distribution of the Chézy parameter C; this distribution can then be input to the nonlinear model to provide accurate results. Thus, the two models, when used in a complementary fashion, can provide a complete, consistent, and self-calibrating method for studying the effects of various natural and manmade phenomena on the lagoon dynamics.

In particular, the two numeric models have been used not only to predict circumstances that can lead to flooding in the city of Venice, but also to evaluate many of the projects proposed to achieve a better hydraulic settlement of the Lagoon of Venice. In fact, it has been determined that although the use of mobile sluices at the inlets of Venice Lagoon will successfully prevent flooding, a permanent but incomplete narrowing of the inlets will not.

# References

- A. Defant, Physical Oceanography, Pergamon Press, Inc., New York, 1961.
- J. J. Dronkers, Tidal Computations in Rivers and Coastal Waters, North-Holland Publishing Co., Amsterdam, 1964.

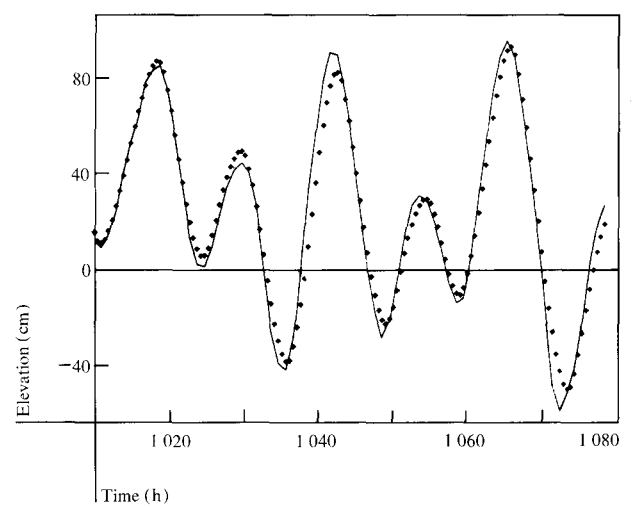


Figure 5 Comparison between observed (continuous line) and computed (dotted line) sea level data in Venice.

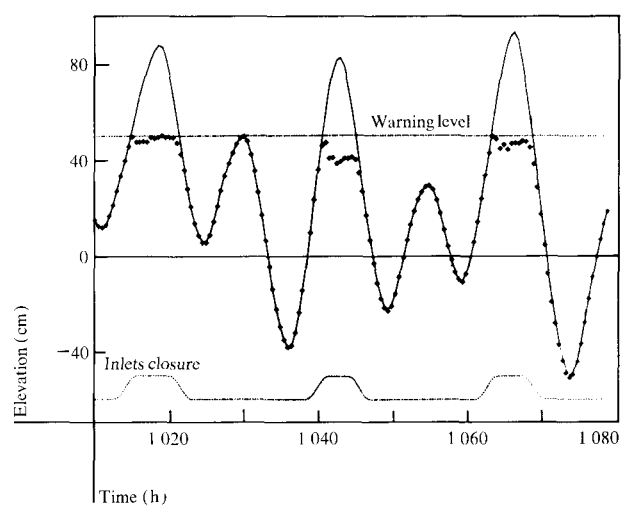


Figure 6 Comparison between computed sea level data in Venice, in absence (continuous line) or in presence (dotted line) of mobile sluices; the warning level and the sluice operating procedure are also shown.

- J. J. Dronkers, "Tidal Computations for Rivers, Coastal Areas, and Seas," J. Hydraul. Div. (ASCE) 95(HY1), 29 (1969).
- H. Lamb, Hydrodynamics, Cambridge University Press, London, England, 1932.
- M. Hendershott and W. Munk, "Tides," Ann. Rev. Fluid Mech. 2, 205 (1970).
- G. I. Marchuk, R. G. Gordeev, and V. Ya. Rivkind, "A Numerical Method for the Solution of Tidal Dynamics Equations and the Results of its Applications," J. Computational Phys. 13, 15 (1973).
- G. I. Taylor, "Tidal Oscillations in Gulfs and Rectangular Basins," Proceedings of the London Mathematical Society, 2nd Series 20, 148 (1922).
- G. I. Marchuk, "About a Numerical Solution of the Poincaré Problem for Ocean Circulation," Dokl. Nauk. SSSR 185, 1047 (1969).

- 9. J. J. Dronkers, "Des Considérations sur la Marée de la Lagune de Venise," Commissione di studio dei provvedimenti per la conservazione e difesa della laguna e della città di Venezia, Rapporti e Studi, Vol. 5, p. 81, Istituto Veneto di Scienze, Lettere ed Arti, Venezia, 1972.
- 10. J. P. Aubin, Approximation of Elliptic Boundary Value Problems, John Wiley & Sons, Inc., New York, 1972.
- 11. J. J. Leendertse, "Aspects of a Computational Model for Long Period Water-Wave Propagation," Report Number RM-5294-PR, Rand Corporation, Santa Monica, CA, 1967.
- 12. J. J. Leendertse, "A Water Quality Simulation Model for Well Mixed Estuaries and Coastal Seas: Vol. 1, Principles of Computation," Report Number RM-6230-RC, Rand Corporation, Santa Monica, CA, 1970.
- 13. W. Hansen, Deut. Hydrog. Z. (Ergaenzungsheft) 1, 1 (1952).
- 14. W. Hansen, "Hydrodynamical Methods Applied to Oceanographic Problems," Proceedings of the Symposium on Mathematical Hydrodynamic Models of Physical Oceanography, Institut fuer Meereskunde der Universitaet Hamburg, 1961, p. 25.
- 15. T. J. Weare, "The Third London Airport Study," J. Hydraul. Res. 15, 55 (1977).
- 16. B. Gustafsson, "An Alternating Direction Implicit Method for Solving the Shallow Water Equations," J. Computational Phys. 7, 239 (1971).
- 17. A. Sielecki and M. G. Wurtele, "The Numerical Integration of the Non-Linear Shallow Water Equations with Sloping Boundaries," J. Computational Phys. 6, 219 (1970).
- R. O. Reid and B. R. Bodine, "Numerical Models for Storm Surges in Galveston Bay," J. Waterways Harbors Div. (ASCE) 94, 33 (1968).
- 19. R. D. Richtmyer and K. W. Morton, Difference Methods for Initial-Value Problems, 2nd ed., Interscience Publishers, New York, 1967.
- 20. W. P. Crowley, "A Global Numerical Ocean Model: Part 1," J. Computational Phys. 3, 111 (1968).
- 21. W. P. Crowley, "A Numerical Model for Viscous, Free-Surface, Barotropic, Wind-Driven Ocean Circulation," J. Com-
- putational Phys. 5, 139 (1970). 22. W. P. Crowley, "A Numerical Model for Viscous, Nondivergent, Barotropic, Wind-Driven Ocean Circulation," J.
- Computational Phys. 6, 183 (1970). 23. C. Taylor and J. Davis, "Tidal and Long-Wave Propagation: A Finite Element Approach," Computers and Fluids 3, 126
- 24. G. Volpi and P. Sguazzero, "La propagazione della marea nella Laguna di Venezia: un modello di simulazione e il suo impiego nella regolazione delle bocche di porto," Rivista Italiana di Geofisica 4, 67 (1977).
- 25. A. Goldmann, R. Rabagliati, and P. Sguazzero, "Propagazione della marea nella Laguna di Venezia: analisi dei dati rilevati dalla rete mareografica lagunare negli anni 1972-73," Rivista Italiana di Geofisica 2, 119 (1975).
- 26. R. Rabagliati and C. Chignoli, "A Two-Dimensional Model for the Lagoon of Venice," Proceedings of the 5th IFIP Optimization Conference 4, 203 (1973).
- 27. A. Goldmann, R. Rabagliati, and P. Sguazzero, "Characteristics of the Tidal Wave in the Lagoon of Venice," Technical Report CRV009/513-3539, IBM Scientific Center, Venice, Italy, December 1975.
- 28. P. Sguazzero, A. Giommoni, and A. Goldmann, "An Empirical Model for the Prediction of the Sea Level in Venice," Technical Report CSV006/513-3515, IBM Scientific Center, Venice, Italy, September 1972.
- 29. C. Chignoli and R. Rabagliati, "Un modello matematico per la Laguna di Venezia," Sistemi ed Automazione 22 (165), 679 (1976).
- 30. P. Pirazzoli, "Inondations et niveaux marins à Venise," Memoires du Laboratoire de Géomorphologie de l'Ecole Pratique de Hautes Etudes, no. 22, Dinard, Paris, 1970.
- 31. R. Dazzi and F. Nyffeler, "Le régime des courants entre le centre historique de Venise et la zone industrielle de Mar-

- ghera," Technical Report 74, Laboratorio Consiglio Nazionale della Ricerche per lo Studio della Dinamica delle Grandi Masse, Venezia, 1973.
- 32. G. Supino, "The Propagation of the Tide Inside a Lagoon," Meccanica 1, 42 (1970).
- 33. G. F. Carrier and H. P. Greenspan, "Water Waves of Finite Amplitude on a Sloping Beach," J. Fluid Mech. 4, 97 (1958).
- 34. J. J. Stoker, Water Waves, Interscience Publishers, New York, 1957.
- 35. J. J. Stoker, "The Formation of Breakers and Bores,"
- Comm. Pure. Appl. Math. 1, 1 (1948).
  36. G. Platzmann, "The Dynamical Prediction of Wind Tides on Lake Erie," Meteorological Monographs, 4(26), American Meteorological Society, September 1963.
- 37. P. J. Roache, Computational Fluid Dynamics, Hermosa Publishers, Albuquerque, 1972.
- 38. J. J. Dronkers, "The Linearization of the Quadratic Resistance Term in the Equations of Motion for a Pure Harmonic Tide in a Sea," Proceedings of the Symposium on Mathematical Hydrodynamic Models of Physical Oceanography, Institut fuer Meereskunde der Universitaet Hamburg, 1961, p. 195.
- 39. K. Kajiura, "A Note on the Generation of Boundary Waves of Kelvin Type," Proceedings of the Symposium on Mathematical Hydrodynamic Models of Physical Oceanography, Institut fuer Meereskunde der Universitaet Hamburg, 1961, p. 135.
- 40. L. Collatz, The Numerical Treatment of Differential Equations, Springer-Verlag, Berlin, 1966.
- 41. R. S. Varga, Matrix Iterative Analysis, Prentice-Hall, Inc., Englewood Cliffs, NJ, 1962.
- 42. D. M. Young, Iterative Solution of Large Systems, Academic Press, Inc., New York, 1972.
- 43. F. G. Gustavson, "Some Basic Techniques for Solving Sparse Systems of Equations," Sparse Matrices and their Applications, D. J. Rose and R. A. Willoughby, eds., Plenum Press, New York, 1972, p. 41.
- 44. J. L. Lions, Contrôle Optimal de Systèmes Gouvernés per des Equations aux Derivées Partielles, Dunod, Gauthier-Villars, Paris, 1968.
- 45. D. Canon, C. D. Cullum, and E. Polak, Theory of Optimal Control and Mathematical Programming, McGraw-Hill Book Co., Inc., New York, 1970.
- 46. R. Fletcher, "Minimizing General Functions Subject to Linear Constraints," Numerical Methods for Non-Linear Optimization, F. A. Lootsma, ed., Academic Press, London, 1972, p. 279.
- 47. P. Sguazzero and G. Volpi, "The Linearization of the Quadratic Resistance Term in the Equation of Motion for a Pure Harmonic Tide in a Canal and the Identification of the Chézy Parameter C," Proceedings of the 8th IFIP Conference on Optimization Techniques, Wuerzburg, Germany, 6, Part 1, 391 (1978).
- 48. R. P. Brent, Algorithms for Minimization without Derivatives, Prentice-Hall, Inc., Englewood Cliffs, NJ, 1973
- 49. A. Tomasin, "Recent Changes in the Tidal Regime in Ven-
- ice," Rivista Italiana di Geofisica 23, 275 (1974).
  50. A. Ghetti, L. D'Alpaos, and R. Dazzi, "La regolazione delle bocche della Laguna di Venezia per l'attenuazione delle acque alte indagata con il metodo statico," Commissione di studio dei provvedimenti per la conservazione e difesa della Laguna e della città di Venezia, Rapporti e Studi, Vol. 5, p. 11, Istituto Veneto di Scienze, Lettere ed Arti, Venezia,
- 51. C. E. Kindswater and R. W. Carter, "Tranquil Flow Through Open-Channel Constrictions," Trans. ASCE 120, 955 (1955).

Received September 2, 1977; revised April 7, 1978

The authors are located at the IBM Italy Scientific Center, Palazzo Giustinian, Dorsoduro 3288, 30123 Venice, Italy.